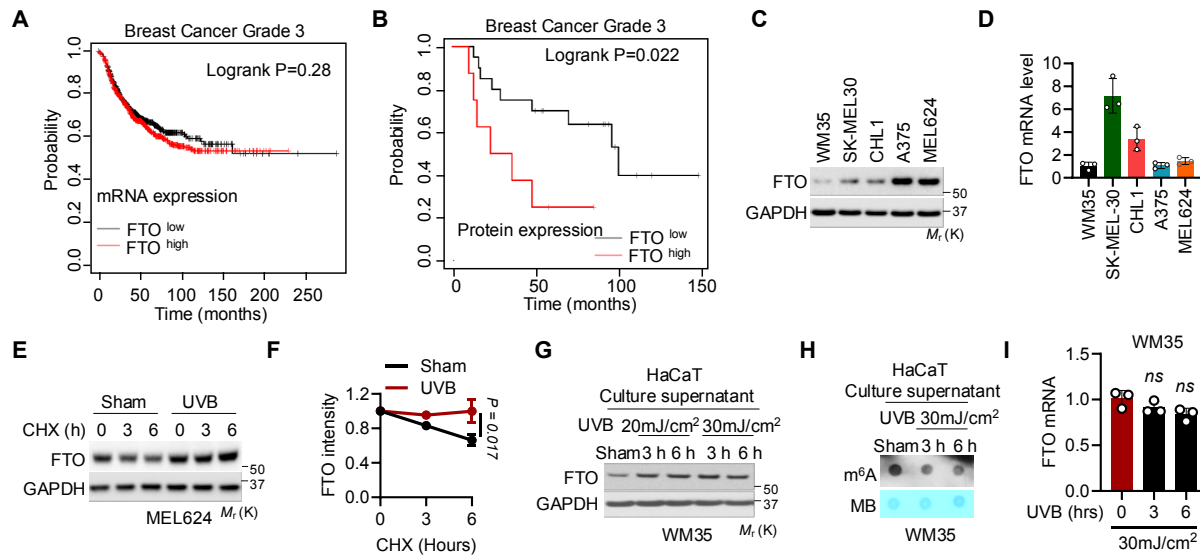


Targeting DTX2/UFD1-mediated FTO degradation to regulate anti-tumor immunity

Cui *et al.*

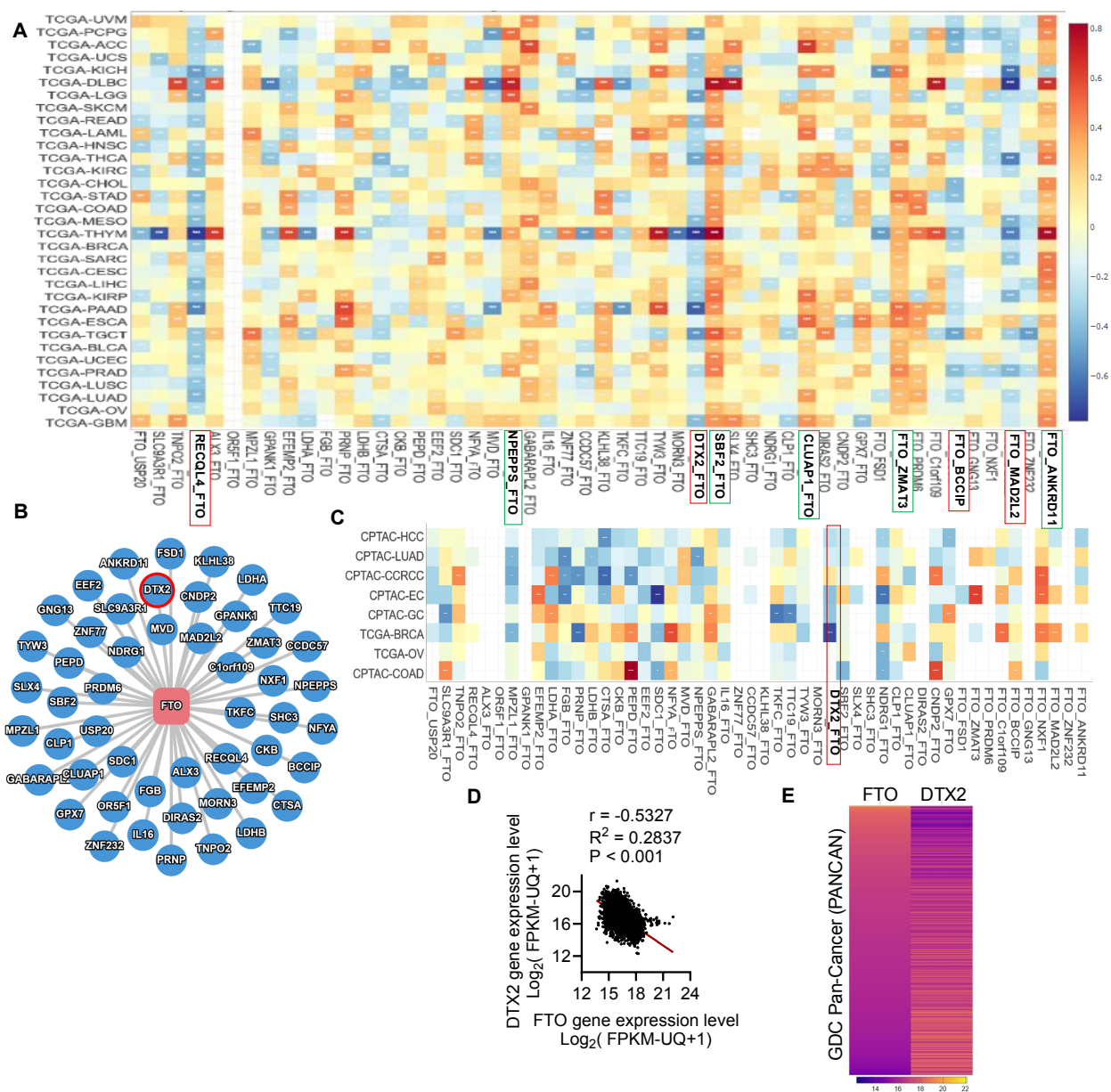
Supplementary figures, figure legends, tables, and detailed methods



Supplementary Figure S1. Related to Figure 1. DTX2 is an E3 ubiquitin ligase for FTO that induces FTO ubiquitination and degradation.

- A.** Overall survival of Grade 3 breast cancer patients with high FTO mRNA level (n = 650) and patients with low FTO mRNA level (n = 650).
- B.** Overall survival of Grade 3 breast cancer patients with high FTO protein level (n = 8) and low FTO protein level (n = 20).
- C.** Immunoblot analysis of FTO and GAPDH in melanoma cell lines.
- D.** qPCR analysis of FTO mRNA levels in melanoma cell lines (n=3).
- E.** Immunoblot analysis of FTO in sham- and UVB-irradiated MEL624 cells treated with cycloheximide (CHX, 100 µg/ml) over a time course.
- F.** Quantification of **E** (n=3).
- G.** Immunoblot analysis of FTO and GAPDH in WM35 cells treated with supernatant from HaCaT cells exposed to sham or UVB irradiation at indicated doses.
- H.** m⁶A dot blot assay in WM35 cells treated with supernatant from sham- or UVB-irradiated HaCaT cells.
- I.** qPCR analysis of FTO mRNA levels in cells as in **G** (n=3).

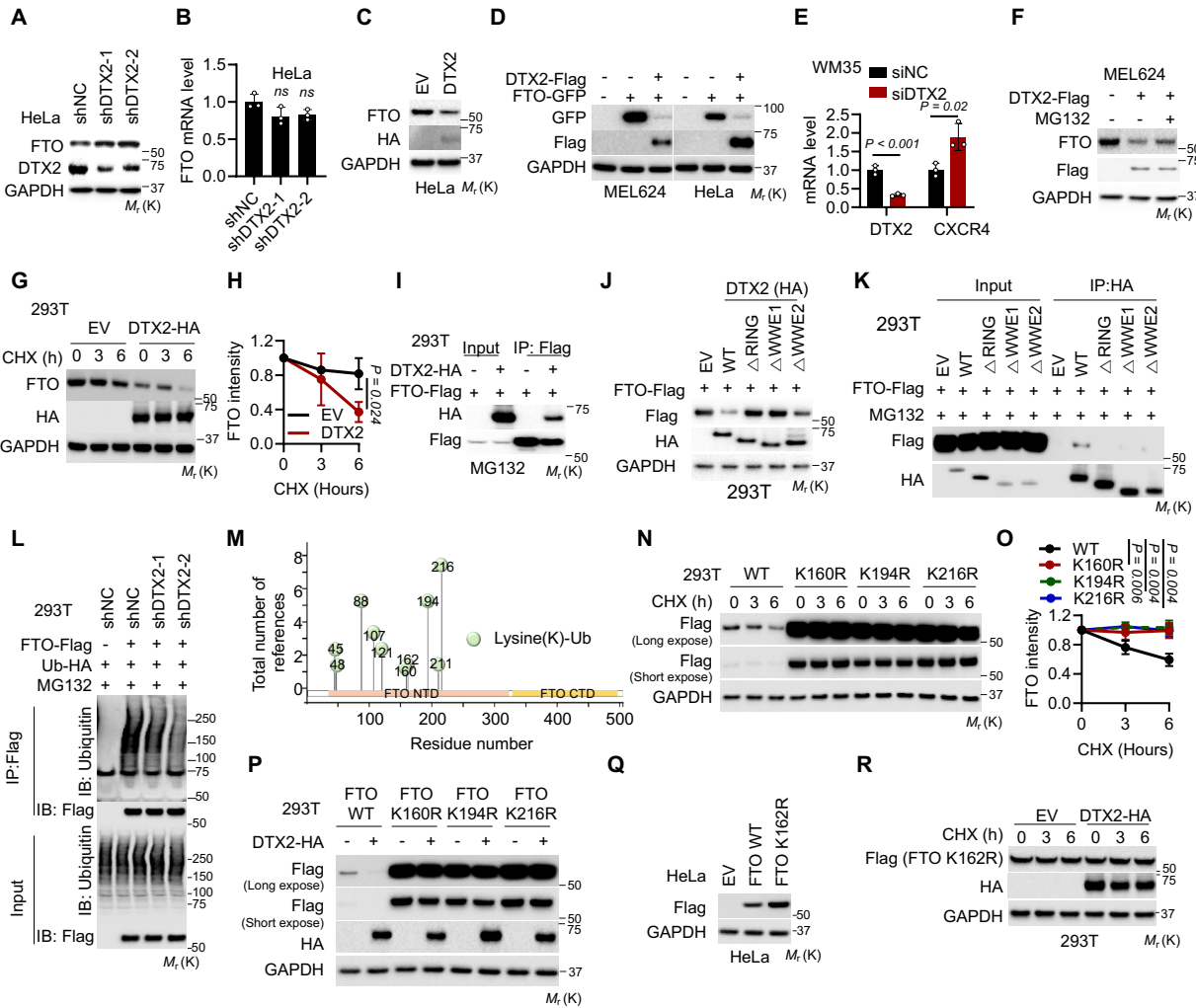
Error bars are shown as mean ± S.D. (D, F, I). p-values are from two-tailed unpaired t-tests (F, I).



Supplementary Figure S2. Related to Figure 1. DTX2 expression was negatively correlated with FTO expression in cancer.

- A.** mRNA correlation of FTO-interacting proteins with FTO across cancer types (PINA).
- B.** Tree graph of FTO-interacting proteins (PINA).
- C.** Correlation of FTO-interacting protein expression with FTO protein level across cancer types (PINA).
- D.** Correlation of DTX2 mRNA level with FTO mRNA level in GDC Pan-Cancers (PANCAN) (n=19189).
- E.** Correlation heatmap of DTX2 gene expression level and FTO gene expression level in GDC Pan-Cancers (PANCAN) (n=19189).

, $P < 0.05$; *, $P < 0.01$, *****, $P < 0.001$ (A, C). P values are from Spearman's correlation test (A, C). Correlation coefficient r and p -value is from Pearson correlation analysis (D).

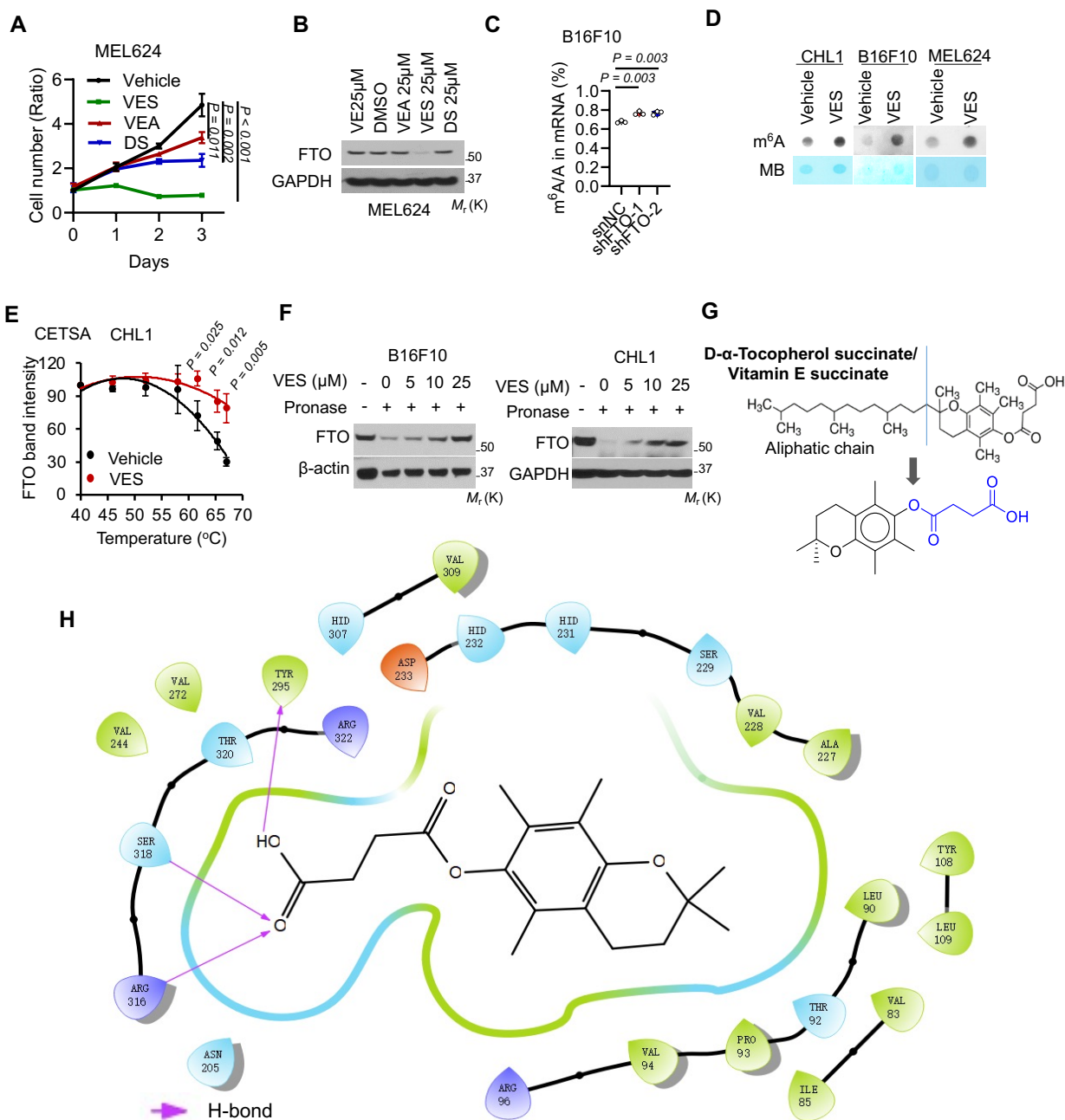


Supplementary Figure S3. Related to Figure 1. DTX2 is an E3 ubiquitin ligase for FTO that induces FTO ubiquitination and degradation.

- A.** Immunoblot analysis of FTO, DTX2, and GAPDH in HeLa cells with or without DTX2 knockdown.
- B.** qPCR analysis of FTO mRNA levels in HeLa cells with or without DTX2 knockdown (n=3).
- C.** Immunoblot analysis of FTO, HA, and GAPDH in HeLa cells with or without DTX2 overexpression.
- D.** Immunoblot analysis of FTO, DTX2, and GAPDH in MEL624 and HeLa cells with or without overexpression of DTX2 and FTO.
- E.** qPCR analysis of CXCR4 mRNA level in WM35 cells with or without DTX2 knockdown (n=3).
- F.** Immunoblot analysis of FTO and DTX2-Flag in MEL624 cells with or without DTX2-Flag overexpression and treated with or without MG132 (10 μ M) for 6 h.
- G.** Immunoblot analysis of FTO in 293T cells transfected with DTX2 and treated with cycloheximide (CHX, 100 μ g/ml) over a time course.
- H.** Quantification of **G** (n=3).

- I.** Co-IP analysis of FTO binding to DTX2 in 293T cells transfected with FTO-Flag and DTX2-HA treated with MG132 (10 μ M) for 6 h.
- J.** Immunoblot analysis of 293T cells transfected with FTO-Flag in combination with empty vector (EV), WT-HA, Δ RING-HA, Δ WWE1-HA, or Δ WWE2-HA.
- K.** Co-IP analysis of FTO binding with WT DTX2 or DTX2 mutants in 293T cells transfected with empty vector (EV), WT-HA, Δ RING-HA, Δ WWE1-HA, Δ WWE2-HA in combination with FTO-Flag and treated with MG132 (10 μ M) for 6 h.
- L.** FTO ubiquitination assay in 293T cells with or without DTX2 knockdown, transfected with Ub-HA and FTO-Flag, and treated with MG132 (10 μ M) for 6 h. Protein lysates were immunoprecipitated with Flag-beads and ubiquitination was detected with the anti-Ubiquitin antibody.
- M.** Lysine ubiquitylation sites in the NTD (N-terminal domain) and CTD (C-terminal domain) of FTO, including K45, K48, K88, K107, K121, K160, K162, K194, K211, and K216 in the NTD.
- N.** Immunoblot analysis of Flag (FTO) in 293T cells transfected with WT, K160R, K194R, and K216R FTO and treated with cycloheximide (CHX, 100 μ g/ml) over a time course.
- O.** Quantification of **N** (n =3).
- P.** Immunoblot analysis of Flag (FTO) and HA (DTX2) in 293T cells transfected with or without DTX2 in combination with WT, K160R, K194R, or K216R FTO.
- Q.** Immunoblot analysis of Flag (FTO) and GAPDH in HeLa cells transfected with Flag-tagged WT and K162R FTO.
- R.** Immunoblot analysis of Flag (FTO-K162R) in 293T cells with or without overexpression of DTX2-HA and Flag-tagged FTO-K162R and treated with cycloheximide (CHX, 100 μ g/ml) over a time course.

Error bars are shown as mean \pm S.D. (B, E, H and O). p-values are from two-tailed unpaired t-tests (B, E, H and O).



Supplementary Figure S4. Related to Figure 2. VES induces FTO protein degradation.

A. Cell proliferation assay in MEL624 cells treated with or without VEA (25 μM; T3376; Sigma), VES (25 μM; T3126; Sigma), or DS (25 μM; W239607; Sigma) (n = 3).

B. Immunoblot analysis of FTO and GAPDH in MEL624 cells treated with or without VEA (25 μM), VES (25 μM), or DS (25 μM).

C. Quantification of the m^6A/A ratios in mRNA by LC-MS/MS in B16F10 cells with or without FTO knockdown (n=3).

D. m^6A dot blot assay in CHL1, MEL624, and B16F10 cells treated with or without VES.

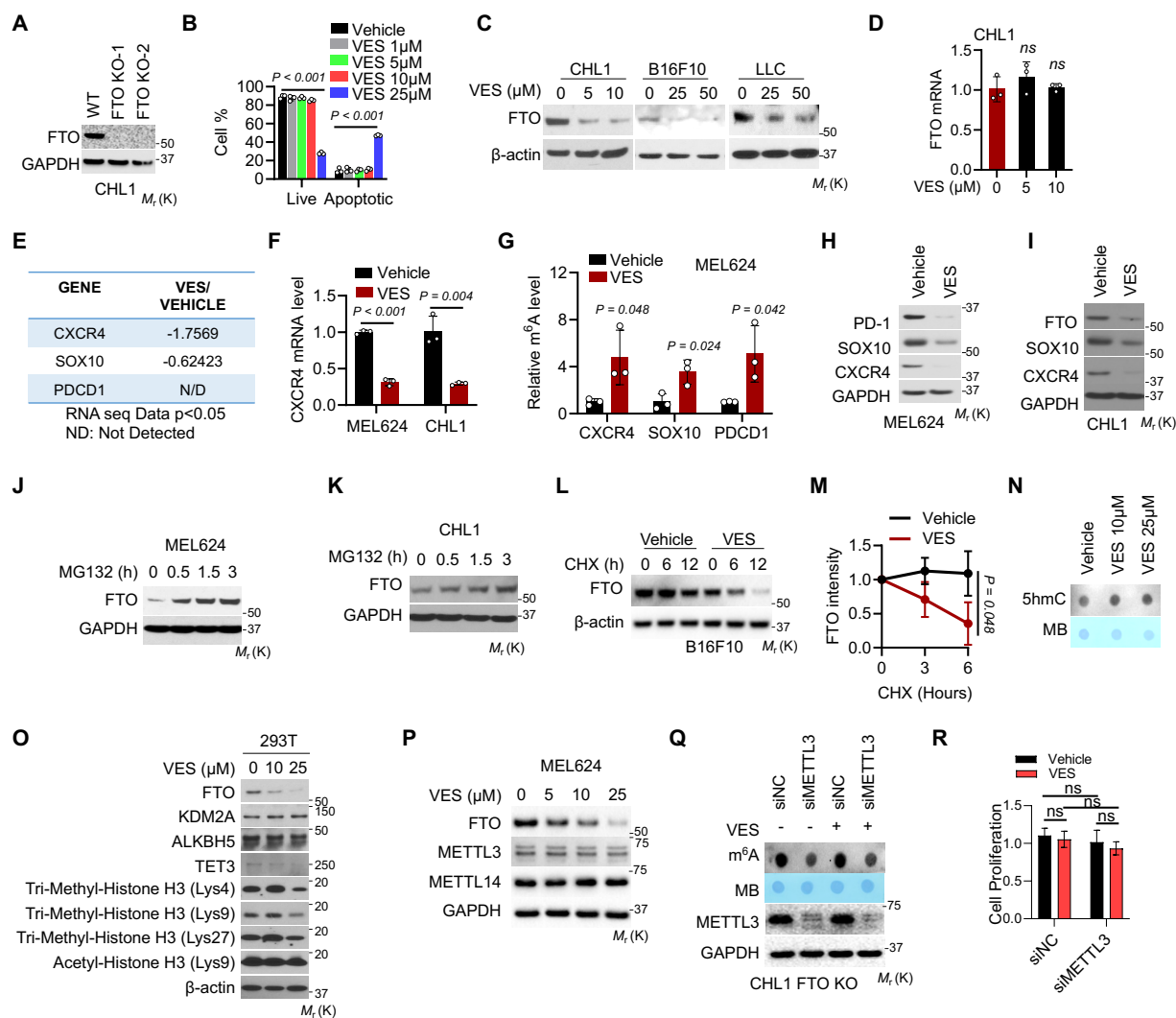
E. Thermal shift curves of FTO from CETSA in CHL1 cells treated with or without VES (10 μ M) (n=3).

F. Immunoblot analysis of FTO from DARTS assay in CHL1 and B16F10 cells treated with or without VES.

G. 2D Chemical structure of VES.

H. 2D ligand interaction diagram for the VES-FTO interaction without VES's aliphatic chain.

Error bars are shown as mean \pm S.E. (A, C, E). p-values are from two-tailed unpaired t-tests (A, C, E).

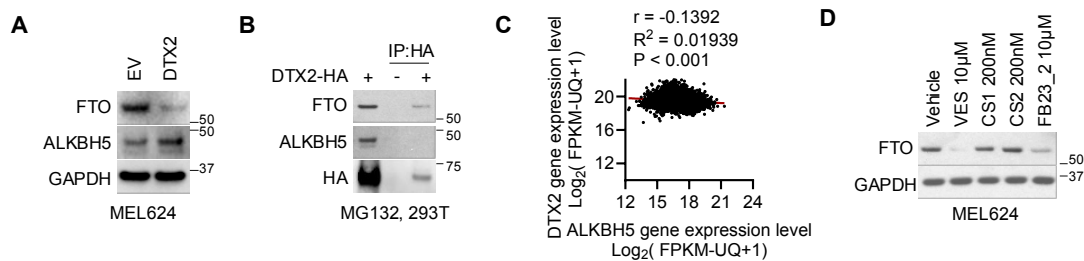


Supplementary Figure S5. Related to Figure 2. VES induces FTO protein degradation.

- Immunoblots analysis of FTO and GAPDH in CHL1 cells with or without FTO deletion.
- Cell viability assay in MEL624 cells treated with VES at different doses for 72 h (n=3).
- Immunoblots analysis of FTO and GAPDH in CHL1, B16F10, and LLC cells treated with VES at different doses for 72 h.
- qPCR analysis of FTO mRNA in CHL1 cells with VES at different doses for 72 h (n=3).
- Altered expression of CXCR4, SOX10, and PDCD1 from RNA-seq analysis in MEL624 cells treated with vehicle or VES (25 μ M) for 72 h.
- qPCR analysis of CXCR4 mRNA level in MEL624 cells and CHL1 cells treated with or without VES 10 μ M for 72 h (n=3).

- G.** m⁶A IP qPCR analysis of m⁶A enrichment in the CXCR4, SOX10, and PDCD1 transcripts in MEL624 cells treated with or without VES 10 μ M for 72 h (n = 3).
- H.** Immunoblot analysis of protein levels of PD-1, SOX10, and CXCR4 in MEL624 cells treated with or without VES 10 μ M for 72 h.
- I.** Immunoblot analysis of protein levels of FTO, SOX10, and CXCR4 in CHL1 cells treated with or without VES 10 μ M for 72 h.
- J.** Immunoblot analysis of FTO and GAPDH in MEL624 treated with MG132 (10 μ M) over a time course.
- K.** Immunoblot analysis of FTO and GAPDH in CHL1 cells treated with MG132 (10 μ M) over a time course.
- L.** Immunoblot analysis of FTO in B16F10 cells treated with or without VES and cycloheximide (CHX, 100 μ g/ml) over a time course.
- M.** Quantification of L (n =3).
- N.** 5hmC dot blot assay in MEL624 cells treated with or without VES for 72 h.
- O.** Immunoblot analysis of indicated proteins in 293T cells treated with or without VES.
- P.** Immunoblot analysis of indicated proteins in MEL624 cells treated with or without VES for 72 h.
- Q.** m⁶A dot blot assay and immunoblot analysis in CHL1 FTO KO cells with or without METTL3 knockdown and VES for 72 h.
- R.** Cell proliferation assay in CHL1 FTO KO cells transfected with or without METTL3 knockdown and VES for 72 h.

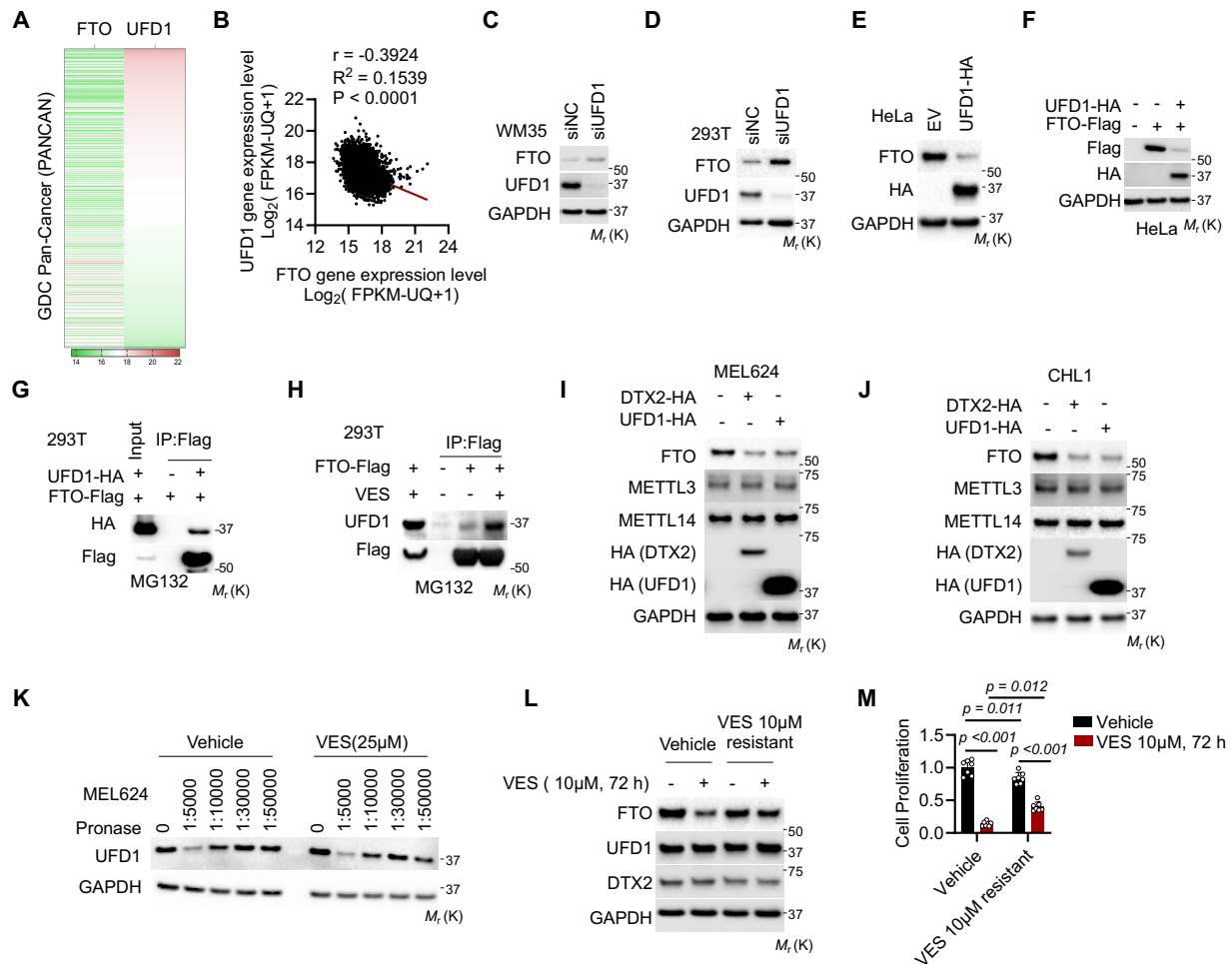
Error bars are shown as mean \pm S.D. (B, D, F, G, M, R). p-values are from two-tailed unpaired t-tests (B, D, F, G, M, R).



Supplementary Figure S6. Related to Figure 3. DTX2 interacts with and down-regulates FTO, but not ALKBH5.

- A.** Immunoblot analysis of FTO, ALKBH5, and GAPDH in MEL624 cells with or without DTX2 overexpression.
- B.** Co-IP analysis of FTO and ALKBH5 binding with DTX2 in 293T cells transfected with DTX2-HA treated with MG132 (10 μ M) for 6 h.
- C.** Correlation of DTX2 gene expression level with ALKBH5 gene expression level in GDC Pan-Cancers (PANCAN) (n=11768).
- D.** Immunoblot analysis of FTO, ALKBH5, and GAPDH in MEL624 cells treated with or without VES, CS1, CS2, and FB23-2 for 72 h.

Correlation coefficient r and p -value is from Pearson correlation analysis (C).



Supplementary Figure S7. Related to Figure 4. UFD1 is required for VES-induced FTO protein degradation.

A. Correlation heatmap of UFD1 mRNA level and FTO mRNA level in GDC Pan-Cancers (PANCAN) (n=19189).

B. Correlation plot of UFD1 mRNA level and FTO mRNA level in GDC Pan-Cancers (PANCAN) (n=19189).

C. Immunoblot analysis of FTO, UFD1, and GAPDH in WM35 cells with or without UFD1 knockdown.

D. Immunoblot analysis of FTO, UFD1, and GAPDH in 293T cells with or without UFD1 knockdown.

E. Immunoblot analysis of FTO, UFD1 (HA), and GAPDH in HeLa cells with or without UFD1 overexpression.

F. Immunoblot analysis of FTO, UFD1 (HA), and GAPDH in HeLa cells with or without overexpression of UFD1 and FTO.

G. Co-IP analysis of the binding of FTO with UFD1 in 293T cells transfected with FTO-Flag and UFD1-HA with MG132 (10 μM) for 6 h.

H. Co-IP analysis of the binding of FTO with UFD1 in 293T cells transfected with FTO-Flag and treated with or without VES with MG132 (10 μ M) for 6 h.

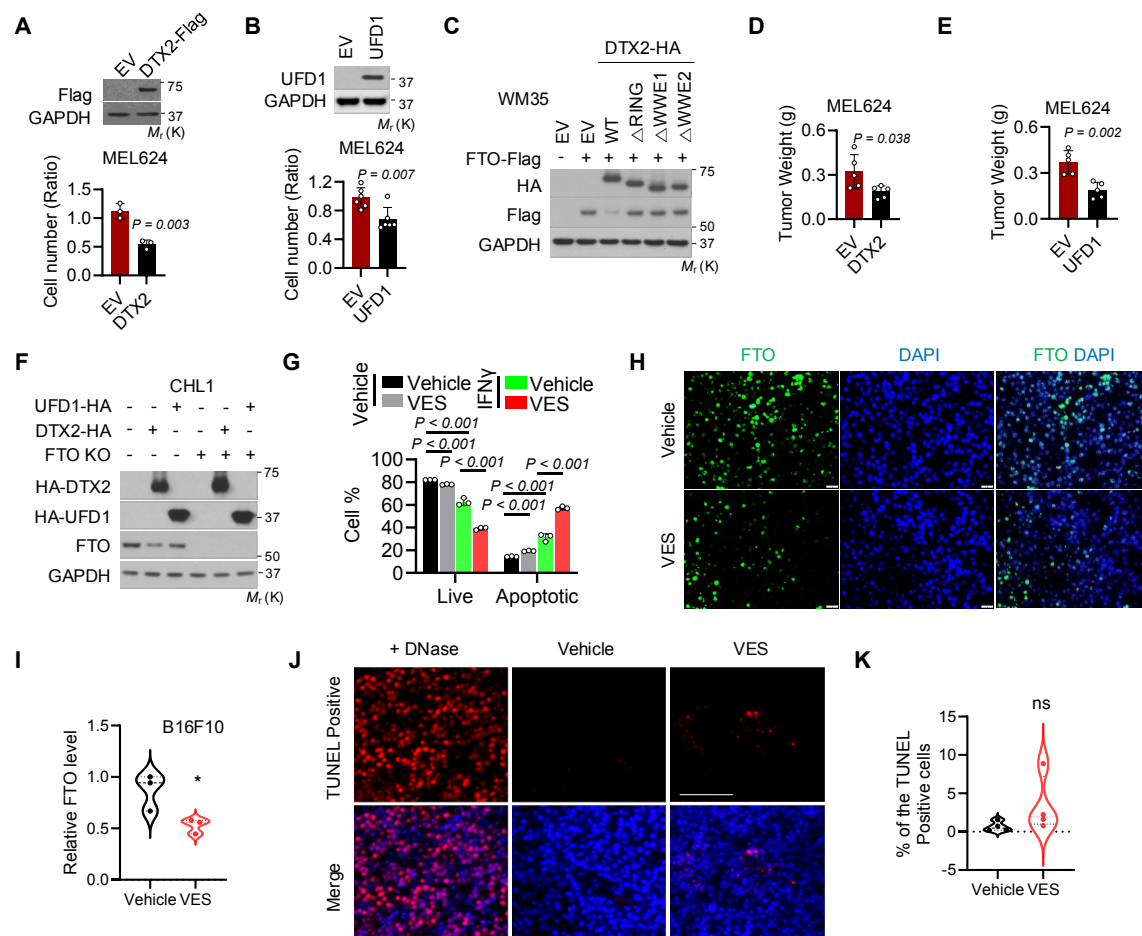
I-J. Immunoblot analysis in MEL624 (**I**) and CHL1 (**J**) cells transfected with or without DTX2 and UFD1.

K. Immunoblot analysis of UFD1 and GAPDH from DARTS assay in MEL624 cells treated with or without VES.

L. Immunoblot analysis of MEL624 cells treated with or without 10 μ M VES for 7 weeks, with additional treatment of 10 μ M VES for 72 h.

M. Cell proliferation assay of MEL624 cells treated with or without 10 μ M VES for 7 weeks, with additional treatment of 10 μ M VES for 72 h.

Error bars are shown as mean \pm S.D. (M). p-values are from two-tailed unpaired t-tests (M). Correlation coefficient r and p-value is from Pearson correlation analysis (B).



Supplementary Figure S8. Related to Figure 5. Effect of targeting FTO degradation on tumor growth and response to immunotherapy.

A. Immunoblot analysis of DTX2 and cell proliferation assay in MEL624 cells with or without DTX2 overexpression (n = 3).

B. Immunoblot analysis of UFD1 and cell proliferation assay in MEL624 cells with or without UFD1 overexpression (n = 6).

C. Immunoblot analysis in WM35 cells with or without overexpression of FTO in combination with overexpression of WT DTX2 and DTX2 mutants related to Fig. 5A.

D. Tumor weight of MEL624 cells with or without DTX2 overexpression in nude mice (n = 5).

E. Tumor weight of MEL624 cells with or without UFD1 overexpression in nude mice (n = 5).

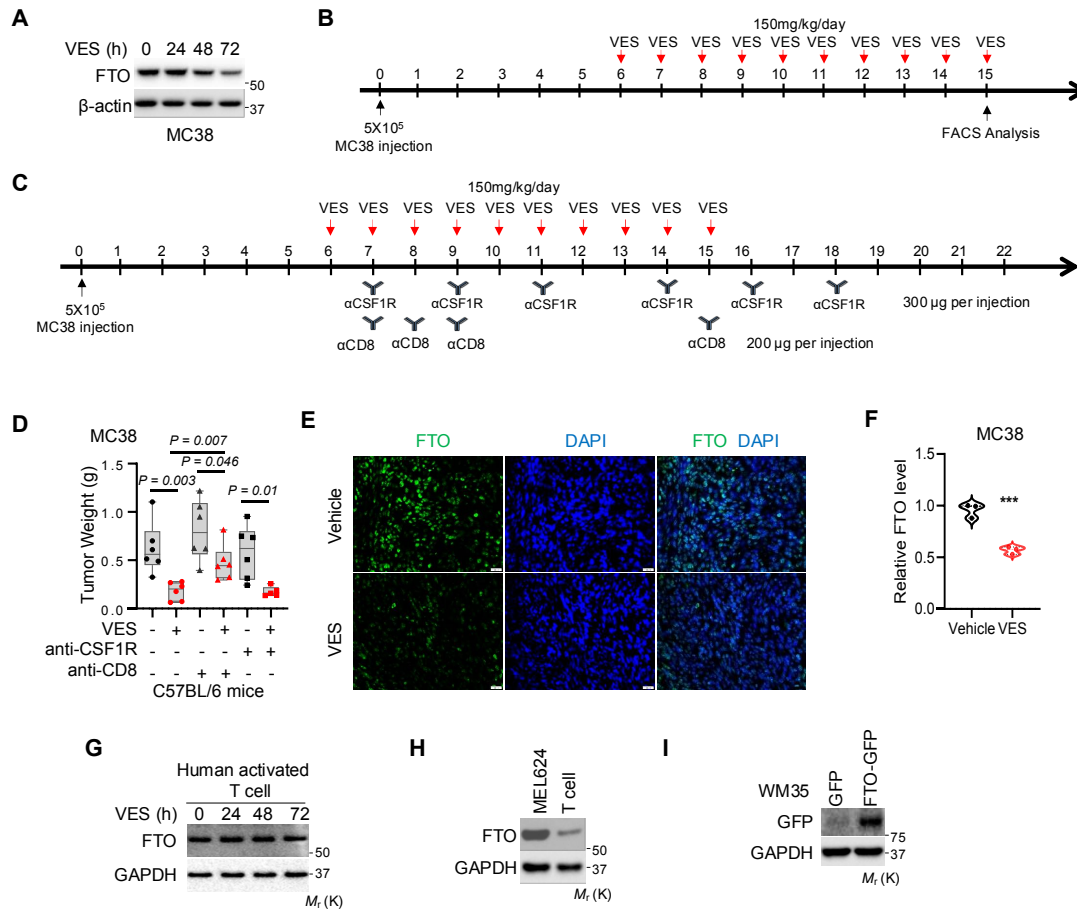
F. Immunoblot analysis in CHL1 cells related to Fig. 5D.

G. Cell viability assay in MEL624 cells treated with or without VES and IFN γ (n=3).

H-I. Immunofluorescence staining of FTO in tumors from mice with subcutaneous injection of B16F10 cells followed by treatment with or without VES (n=3). Scale bar: 20 μ m.

J-K. Apoptosis of tumor tissues in tumors as in H using the TUNEL assay (n=4). Scale bar: 200 μ m.

Error bars are shown as mean \pm S.D. (A-B, D-E, G, I, K). p-values are from two-tailed unpaired t-tests (A-B, D-E, G, I, K).



Supplementary Figure S9. Related to Figure 6. VES increased T cell-mediated cytotoxicity by targeting FTO.

A. Immunoblot analysis of FTO and β -actin in MC38 cells treated with VES (25 μ M) over a time course.

B. A schematic diagram of experimental design for VES treatment for Fig. 6A-H.

C. A schematic diagram of experimental design and VES, anti-CD8, and anti-CSF1R antibody treatment schedule for Fig. 6I and Fig. S9D-F.

D. Tumor weight of MC38 tumors in C57BL/6 mice treated with or without VES in combination with the anti-CD8, anti-CSF1R, or isotype control antibody.

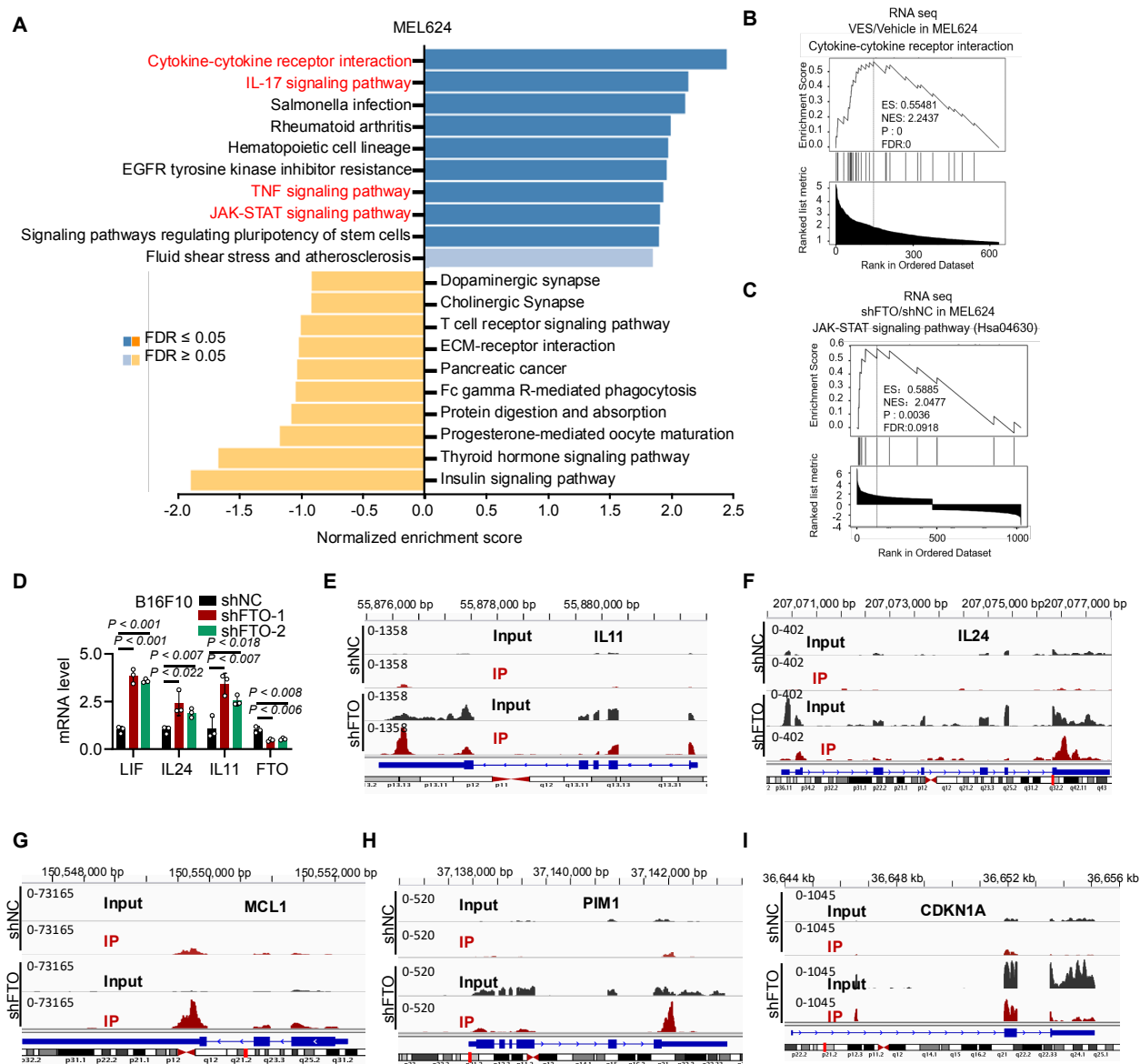
E, F. Immunofluorescence staining of FTO in tumors from mice with subcutaneous injection of MC38 cells followed by treatment with or without VES (n=3). Scale bar: 20 μ m.

G. Immunoblot analysis of FTO and GAPDH in activated human T cells.

H. Immunoblot analysis of FTO and GAPDH in MEL624 cells and human activated T cells.

I. Immunoblot analysis of FTO-GFP and GAPDH in WM35 cells with or without FTO overexpression.

Error bars are shown as mean \pm S.D. (D, F). p-values are from two-tailed unpaired t-tests (D, F).



Supplementary Figure S10. Related to Figure 7. FTO knockdown increases m⁶A enrichment across the LIF transcript.

A. Pathway analysis of the differentially expressed genes from RNA seq analysis of MEL624 cells treated with or without VES.

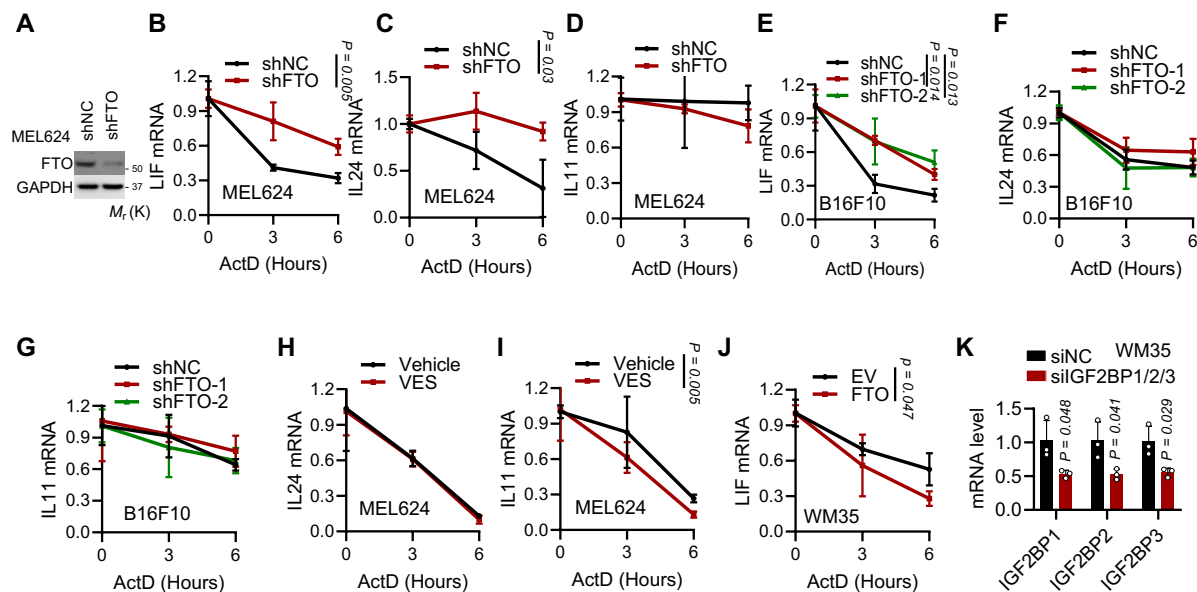
B. Gene set enrichment analysis (GSEA) of the cytokine-cytokine receptor pathway in MEL624 cells treated with or without VES.

C. GSEA of the JAK-STAT signaling pathway in MEL624 cells with or without FTO knockdown.

D. qPCR analysis of the mRNA levels of genes indicated in B16F10 with or without FTO knockdown (n=3).

E-I. Distribution of m⁶A peaks for genes indicated in MEL624 cells with or without FTO knockdown.

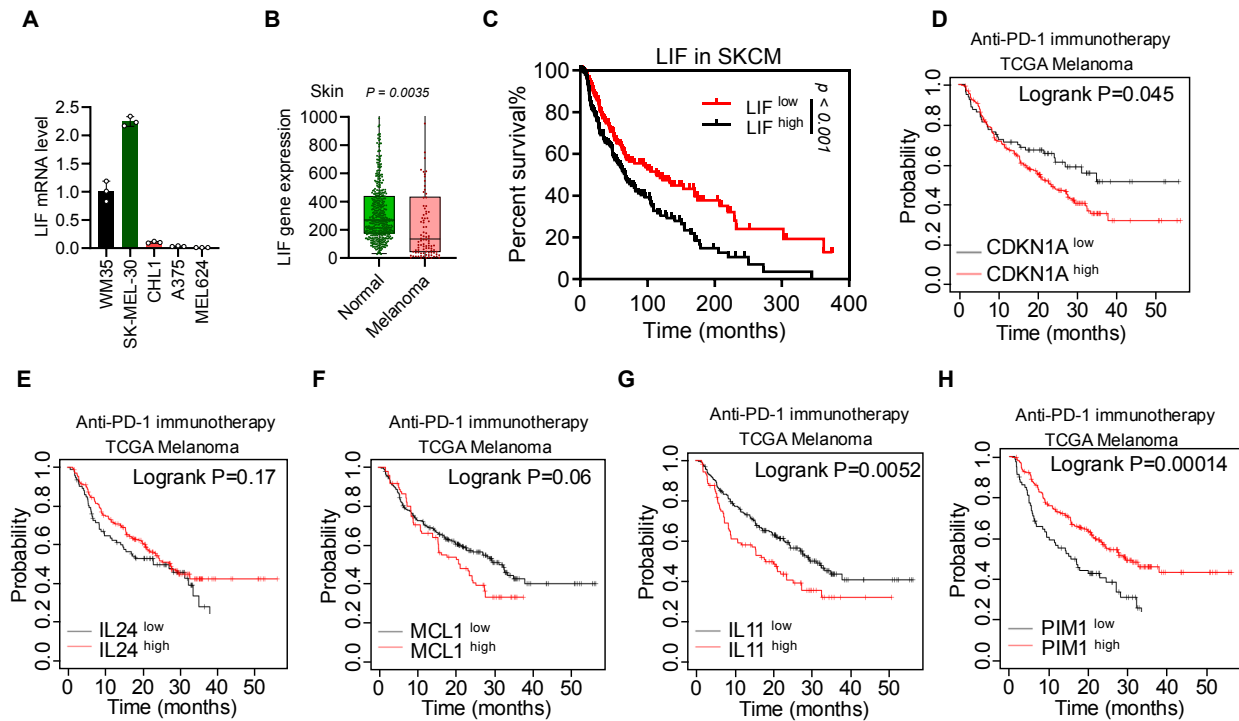
Error bars are shown as mean \pm S.D. (D). p-values are from two-tailed unpaired t-tests (D).



Supplementary Figure S11. Related to Figure 7. FTO inhibition enhances T cell-mediated cytotoxicity by targeting LIF.

A. Immunoblot analysis of FTO level in MEL624 cells with or without FTO knockdown.
B-D. qPCR analysis of LIF, IL24, and IL11 mRNA stability following treatment with actinomycin D (ActD, 2 μ M) in MEL624 cells with or without FTO knockdown (n = 3).
E-G. qPCR analysis of LIF, IL24 and IL11 mRNA stability following treatment with actinomycin D (ActD, 2 μ M) in B16F10 cells with or without FTO knockdown (n = 3).
H-I. qPCR analysis of IL24 and IL11 mRNA stability following treatment with actinomycin D (ActD, 2 μ M) in MEL624 cells with or without VES treatment for 72 h (n = 3).
J. qPCR analysis of LIF mRNA stability following treatment with actinomycin D (ActD, 2 μ M) in WM35 cells with or without FTO overexpression (n = 3).
K. qPCR analysis of indicated gene expression in WM35 cells with or without IGF2BP1/2/3 knockdown (n = 3).

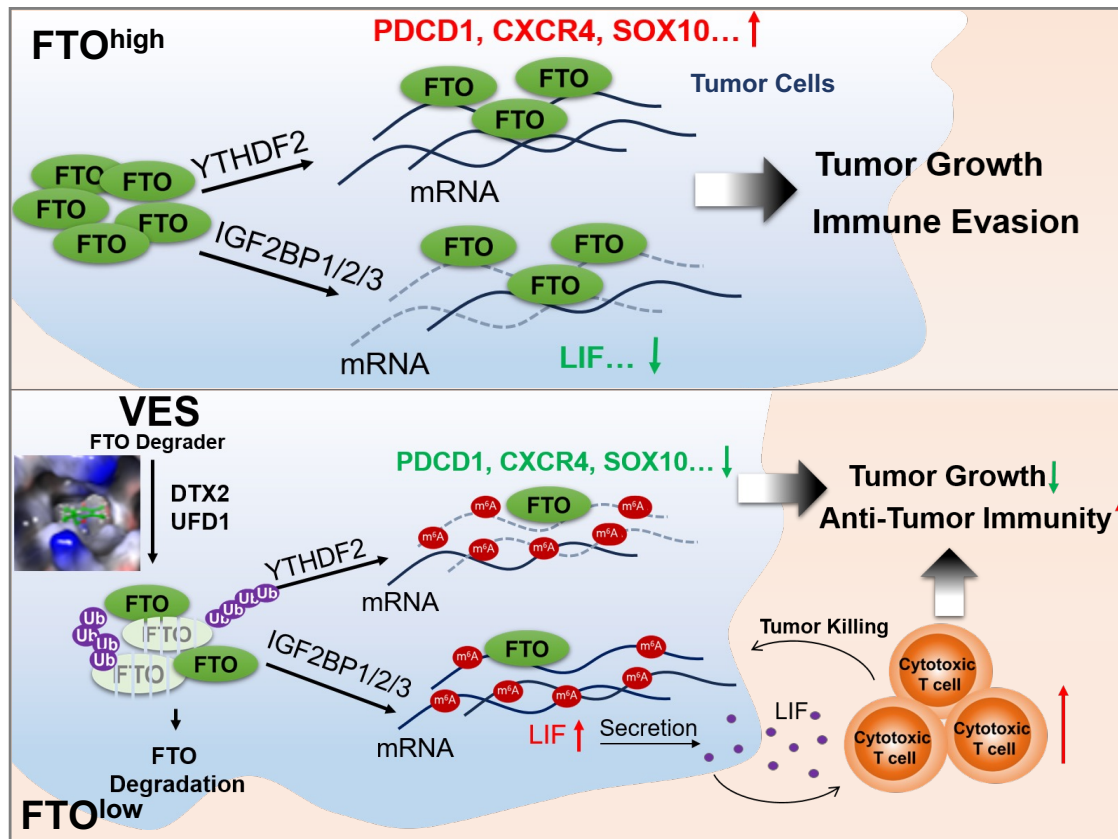
Error bars are shown as mean \pm S.D. (B-K). p-values are from two-tailed unpaired t-tests (B-K).



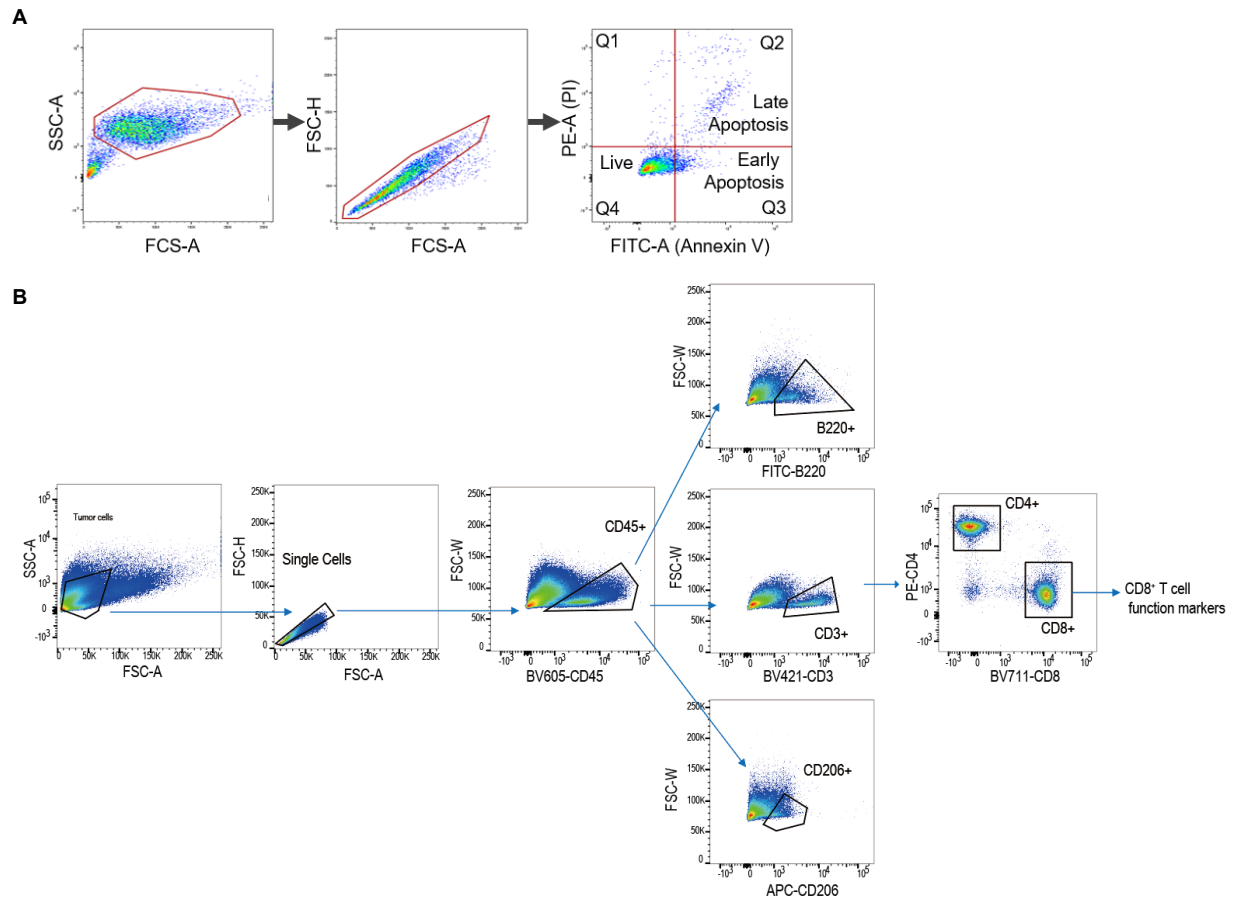
Supplementary Figure S12. Related to Figure 7. FTO inhibition enhances T cell-mediated cytotoxicity by targeting LIF.

- A.** qPCR analysis of LIF mRNA levels in melanoma cell lines.
- B.** Boxplot showing gene expression of LIF in normal human skin and cutaneous melanoma.
- C.** Overall survival of cutaneous melanoma patients with high LIF mRNA level (n =229) and low LIF mRNA level (n =229).
- D.** Overall survival of melanoma patients with high CDKN1A mRNA level (n =233) and low CDKN1A mRNA level (n =92) following anti-PD-1 immunotherapy.
- E.** Overall survival of melanoma patients with high IL24 mRNA level (n =233) and low IL24 mRNA level (n =92) following anti-PD-1 immunotherapy.
- F.** Overall survival of melanoma patients with high MCL1 mRNA level (n = 96) and low MCL1 mRNA level (n =229) following anti-PD-1 immunotherapy.
- G.** Overall survival of melanoma patients who had high IL11 mRNA level (n =105) and low IL11 mRNA level (n =220) following anti-PD-1 immunotherapy.
- H.** Overall survival of melanoma patients with high PIM1 mRNA level (n =248) and low PIM1 mRNA level (n =80) following anti-PD-1 immunotherapy.

Error bars are shown as mean \pm S.D. (A). p-value is from a two-tailed unpaired t-test (B).



Supplementary Figure S13. Schematic summary for the regulatory and functional role of targeting FTO protein degradation in anti-tumor immunity and response to immunotherapy.



Supplementary Figure S14. Gating strategy for flow cytometric analysis of immune cell profiling.

Supplementary Table S2 Primer list

Gene name	Forward (5' to 3')	Reverse (5' to 3')
IGF2BP1(human)	atccgcaacatcacaaaaca	attatgggccaggatcttcag
IGF2BP2(human)	ccggaaagaacatcactgt	aagagtgatgatgcgggaac
IGF2BP3(human)	agttgtgtccctcgtgacc	gtccactttgcagagccttc
GAPDH(human)	agggctgctttaactctggt	cccacttgatttggaggga
FTO(human)	acttggtcccttatctgacc	tgtgcagtgtgagaaggctt
DTX2(human)	gccagtgtactctccagac	gcggtccatctctgtctgt
CDKN1A(human)	ccaagctctacttccac	ctgagagtctccaggccac
MCL1(human)	gccaaaggacacaagccaat	atgcaaaccagctctact
PIM1(human)	ccgagtgtatagccctccag	gggccaagcaccatctaag
IL24(human)	gtggactttagccagcaagc	gttgaatgctctccgaat
IL 11(human)	cttcctgaagaccctggag	gtcttcagcagcagcagtc
LIF(human)	gttccccacaacctggac	ggggtgaggatctctgtgt
SOX10(human)	agcccagggtgaagacagaga	atagggctctgagggctgat
IL11(Mouse)	tgacggagatcacagtctgg	Gagctgtaacggcgaggta
IL24(Mouse)	ttaggacctagcaggagca	Agaaccaccctgtcacttg
LIF(Mouse)	ggcaacctcatgaaccagat	Accatccgatacagctccac
FTO(Mouse)	tcacagcctcggtttagttc	gcaggatcaaaggatttcaacg
△RING-DTX2	aagtgtccccagatgaggacacatctatggagagaagac	gtcttctctccatagatgggtctctcatctgggggcactt
△WWE1-DTX2	ccatggcccaagcccttcccactgttccccagcactc	gagtgtgggggaacagggtggaagggttggggccatgg
△WWE2-DTX2	ccatgcgggctgtgcggagacaagcagggccgccttacc	gggtaaggcgccctgctgtctccgcacagcccgcattg
FTO K121R	acgggtcccctggccagtgcaggggtctaat	attagaccctctcactggccaggggaccgt
FTO K160R	tgaagaacttgcgtccagagagaaggctaagag	ctcattagccttctcttggcagcaagttctcca
FTO K162R	ggaagaacttgcgtccaaagagagggctaagagga	tcctcattagccctctcttggcagcaagttctcc
FTO K194R	ggacaagatgaagtggacattaggagcagagcagc	gctgctctgctcctaagtcacttcatctgtcc
FTO K211R	gaatttcattgatcctcagagaatgccatacctgaaagagg	cctcttcaggatggcattctctgaggatccatgaaattc
FTO K216R	gatcctcagaaaatgccatacctgagagaggaaacattat	ataagggtcctctcaggtatggcattttctgaggatc
FTO R316Q	gccgggtcacaaacctcagtttagttccaccac	gtgggtggaactaaactgaggtgtgaaccggc
FTO S318A	gggtcacaaacctcggtttgcttcacccaccgagtg	cactcggtgggtggaagcaaacaggaggtgtgaacc
FTO Y295F	cttcaccaaggagactgcttttcatgcttgatgatctc	gagatcatcaagcatgaaaaagcagtcctctgtgtgaag

Supplementary Table S3. Antibody list

Antibody	Vendor	Cat	Ratio
anti-m ⁶ A	Synaptic system	202 003	1:2000
anti-FTO	Santa Cruz	SC-271713	1:500
anti-GAPDH	Santa Cruz	sc-47724, sc-32233	1:5000
anti-β-actin	Santa Cruz	SC-47778	1:5000
anti-ALKBH5	Millipore Co	ABE 1013	1:2000
anti-HA	Santa Cruz	sc-7392	1:5000
anti-IGF2BP1	Cell Signaling Technology	8482	1:1000
anti-IGF2BP2	Cell Signaling Technology	14672	1:1000
anti-IGF2BP3	Cell Signaling Technology	57145,	1:1000
Rabbit Anti-Mouse IgG (Light Chain Specific) (D3V2A) mAb (HRP Conjugate)	Cell Signaling Technology	58802	1:5000
Mouse Anti-Rabbit IgG (Conformation Specific) (L27A9) mAb (HRP Conjugate)	Cell Signaling Technology	5127	1:5000
anti-HA	Cell Signaling Technology	3724	1:2000
anti-GFP	abcam	ab290	1:5000
anti-PD-1	Proteintech	66220-I-Ig	1:1000
anti-SOX10	Santa Cruz	SC-365692	1:500
anti-CXCR4	Santa Cruz	SC-53534	1:500
anti-Flag	Cell Signaling Technology	14793S	1:5000
anti-Ubiquitin	Santa Cruz	sc-8017	1:500
anti-KDM2A	Protein tech	24311-1-AP	1:1000
anti-TET3	GeneTex	GTX121453	1:1000
anti-ALKBH5	Millipore	ABE547	1:1000
anti-KDM4A	Proteintech	24943-1-AP	1:1000
anti-METTTL3	Proteintech	15073-1-AP	1:2000
anti-METTTL14	Sigma-Aldrich	HPA038002	1:2000
anti-Tri-Methyl-Histone H3 (Lys4)	Cell Signaling Technology	9751S	1:1000
anti-Tri-Methyl-Histone H3 (Lys9)	Cell Signaling Technology	13969S	1:1000
anti-Tri-Methyl-Histone H3 (Lys27)	Cell Signaling Technology	9733	1:1000
anti-Acetyl-Histone H3 (Lys9)	Cell Signaling Technology	9649S	1:1000
anti-UFD1	Santa Cruz	sc-377265	1:500
anti-DTX2	Proteintech	67209-1-Ig	1:1000
anti-DTX2	abcam	ab170907	1:1000

Experimental Procedures

Cell culture

HaCaT human keratinocytes were kindly provided by Dr. Fusenig, WM35 cells were kindly provided by Dr. Meenhard Herlyn (Wistar Institute, Philadelphia, PA). LLC (murine primary Lewis lung carcinoma), MC38 (murine colon adenocarcinoma cell), HeLa (Human Adenocarcinoma), HEK-293T (human embryonic kidney), A375 (human Melanoma), MEL624 (human Melanoma), CHL-1 (human Melanoma), SK-MEL30 (human Melanoma) and B16F10 (murine Melanoma) cells were purchased from ATCC or provided by the Comprehensive Cancer Center Core Facilities at the University of Chicago. All cells were maintained in DMEM (Dulbecco's modified Eagle's medium) medium (Invitrogen) supplemented with fetal bovine serum (FBS, 10% HyClone), penicillin (100 U/ml), and streptomycin (100 µg/ml, Invitrogen, Carlsbad, CA).

Mouse tumorigenesis and treatment

All the animal procedures used were approved by the institutional animal care and use committee at the University of Chicago. Nude mice were purchased from Harlan Sprague-Dawley; C57BL/6 mice were obtained from Envigo. For xenograft experiments, one million transfected MEL624 cells were injected subcutaneously into the right flanks of 6-week-old female nude mice. Tumor growth was monitored and measured by a caliper, and tumor volume was calculated using the formula $\text{Tumor volume (mm}^3\text{)} = d^2 \times D/2$, where d and D are the shortest and the longest diameters, respectively. For treatment with anti-PD-1 antibody (BioXCell, clone RMP1-14) or isotype control IgG antibody (BioXCell, clone 2A3), B16F10 melanoma cells (5×10^5) were inoculated subcutaneously into C57BL/6 mice. When the tumors reached a volume of 80–100 mm³, mice were treated with anti-PD-1 or isotype control antibody (200 µg/mouse) by intraperitoneal injection three times at intervals of every other day. Treatments with either 150 mg/kg VES (1, 2) (T3126, Sigma; D- α -Tocopherol succinate; in olive oil) or vehicle (DMSO; D8418, Sigma; in olive oil) were started on Day 3 and given daily for 10 days by intraperitoneal injection. For anti-CD8 antibody (BioXCell, BE0061, Clone 2.43), anti-CSF1R antibody (BioXCell, BE0213, clone AFS98), and mouse IgG2b isotype control (BioXCell, BE0086, MPC-11) blockade treatment, MC38 cells (5×10^5) were inoculated subcutaneously into C57BL/6 mice. After tumor cell inoculation, C57BL/6 mice were treated with anti-CD8 antibody on Day 7, 8, 9, and 15 using 200 µg per injection, and with anti-CSF1R antibody on Day 7, 9, 11, 14, 16, and 18 using 300 µg per injection.

Lentiviral generation and infection

Lentiviral constructs were co-transfected with pCMVdelta8.2 packaging plasmid and pVSV-G envelope plasmid into HEK-293T (human embryonic kidney) cells using GenJet™ Plus DNA In Vitro Transfection Reagent (SignaGen Laboratories, SL100499) to generate lentiviral constructs. The virus-containing supernatant was collected at 72 hours. Target cells were infected in the presence of Polybrene (8 µg/ml) (Sigma-Aldrich, St. Louis, MO) and selected with appropriate antibiotics for 7–14 days (3, 4). Lentiviral constructs are as follows: Empty vector (EV) and DTX2-Flag (Origene); EV and UFD1-HA (AbmGood); GFP and FTO-GFP (Genecopoeia); EV and LIF1 (Genecopoeia); pLKO.1 Lentiviral vectors expressing shRNA targeting negative control (shNC), FTO (shFTO), DTX2 (shDTX2), and LIF (shLIF) (Sigma).

Plasmids

pLKO.1 Lentiviral vectors expressing shRNA targeting negative control (shNC), FTO (shFTO), DTX2 (shDTX2), and LIF (shLIF) for humans or mice were purchased from Sigma.

Plasmids used were as follows: lentiviral empty vector (Cat# ExNeg Lv122) and FTO-GFP vector (Cat# EX-H1661-Lv122) were purchased from Genecopoeia; empty vector (Cat# CV012) and FTO-Flag vector (Cat# HG12125-CF) were purchased from SinoBiological; lentiviral

empty vector (pReceiver-Lv157) and LIF (EX-G0101-Lv157) were purchased from Genecopiea; pLenti-HA-Ub plasmid was purchased from Addgene (#74218, kindly provided by Melina Fan); pRK5-HA-Ubiquitin-K48R was purchased from Addgene (#17604, a gift from Ted Dawson); Lentiviral empty vector (Cat# PS100092) and DTX2 with a Flag- and Myc tag (Cat# RC212997L3) were purchased from Origene. Lentiviral empty vector (Cat# Lv587) and UFD1 with a HA tag (Cat# 49091061) were purchased from AbmGood. UFD1 with HA tagging was subcloned into the pcDNA4 vector (Addgene plasmid #28027, kindly provided by Qing Zhong). Point mutants of FTO (K121R, K160R, K162R, K194R, K211R, K216R, R316Q, S318A, Y295F) were generated in the FTO-Flag vector (Cat# HG12125-CF) using a QuikChange Lightning Site-Directed Mutagenesis Kit according to the manufacturer's instructions. The DTX2 (NM_001102594) gene with the HA tag was subcloned into the pcDNA4 vector (Addgene plasmid #28027, kindly provided by Qing Zhong). DTX2 (NM_001102594) domain deletion mutants Δ WWE1, Δ WWE2, and Δ RING with HA tag were subcloned into the pcDNA4 vector (Addgene plasmid #28027, kindly provided by Qing Zhong). The vector for FTO knockout using the CRISPR method was described previously (3). The guide RNA sequences were FTO KO-1: GAAGCGCACCCCGACTGCCG; FTO KO-2: ACGGTCCCCTGGCCAGTGAA. Primers for cloning are shown in Supplementary Table 2.

siRNA transfection

Cells were transfected with siRNA targeting negative control (siNC) (Horizon Discovery Ltd, D-001810-10-20), UFD1 (Horizon Discovery Ltd, L-017918-00-0005), DTX2 (Horizon Discovery Ltd, L-007114-00-0005), IGF2BP1 (Horizon Discovery Ltd, L-003977-00-0005), siRNA targeting IGF2BP2 (Horizon Discovery Ltd, L-017705-00-0005), and/or IGF2BP3 (Horizon Discovery Ltd, L-003976-00-0005) using GenMute™ siRNA Transfection Reagent (Signagen, Ijamsville, MD) according to the manufacturer's instructions.

Quantitative real-time PCR (qPCR)

Quantitative real-time PCR assays were performed using a CFX Connect real-time system (Bio-Rad, Hercules, CA) with Bio-Rad iQ SYBR Green Supermix (Bio-Rad, Hercules, CA). Preparation of cDNA using iScript Reverse Transcription Supermix for RT-qPCR (Bio-Rad, Hercules, CA) for mRNAs. The threshold cycle number (CQ) for each sample was determined in triplicate. The CQ values for FTO, DTX2, IL11, IL24, LIF, CDKN1A, MCL1, PIM1, CXCR4, SOX10 and PDCCD1 were normalized against GAPDH. Primers are shown in Supplementary Table 2.

Quantitative analysis of the m⁶A levels in mRNA

Total RNA was extracted from cells using TRIzol according to the manufacturer's instructions. The quantification of m⁶A in polyadenylated RNA was performed using an Agilent 6460 LC-MS/MS spectrometer, as described previously (5, 6).

m⁶A dot blot assay

Total RNA was isolated with an RNeasy plus Mini Kit (QIAGEN, Hilden, Germany) according to the manufacturer's instructions. RNA samples were loaded onto the Amersham Hybond-N+ membrane (GE Healthcare, Chicago, IL) and UV cross-linked twice to the membrane. The membrane was blocked with 5% BSA (in 1× PBST) for 1 h and incubated with a specific anti-m⁶A antibody (Synaptic Systems, Cat # 202003, Goettingen, Germany) overnight at 4 °C. Next, the membrane was incubated with the HRP-conjugated anti-rabbit IgG (Invitrogen, Cat# 31460) for 1 h at room temperature, and then developed with Thermo ECL SuperSignal Western Blotting Detection Reagent (Thermo Fisher Scientific, Waltham, MA) (3, 4).

5hmC dot blot assay

Total DNA was isolated using the QIAamp DNA Mini Kit (QIAGEN, Hilden, Germany, catalog number 51306) according to the manufacturer's instructions. DNA was treated with RNase A for

1 h at room temperature and then purified. DNA was then denatured by heating at 98°C for 10 min, spotted on Amersham Hybond-N + membrane (GE Healthcare, Chicago, IL, USA), and subsequently UV cross-linked to the membrane twice. Membranes were blocked with 5% BSA (in 1× PBST) for 1 h and then incubated with specific 5hmC (Activity Motif, Cat. No. 39069) overnight at 4 °C. Next, the membrane was incubated with HRP-conjugated rabbit IgG (Invitrogen, Cat. No. 31460) for 1 h at room temperature and then developed with Thermo ECL.

Gene-specific m⁶A qPCR

Total RNA was isolated using the RNeasy Plus Mini Kit (Qiagen). RNA was prepared for input sample and m⁶A immunoprecipitation as follows. RNA was diluted into IP buffer (150 mM NaCl, 0.1% NP-40, 10 mM Tris, pH 7.4, 100 U RNase inhibitor) with the m⁶A antibody (Synaptic Systems, Cat # 202003, Goettingen, Germany), incubated and rotated at 4°C for 2 h, then BSA-coated Dynabeads® Protein A (Thermo Fisher Scientific, Waltham, MA) was added to the solution and it was rotated for an additional 2 h at 4°C. RNA was eluted using Elution buffer (5 mM Tris-HCl pH 7.5, 1 mM EDTA pH 8.0, 0.05% SDS, and 4.2 µl Proteinase K (20 mg/ml)) after being washed with IP buffer. The final eluted mRNA was concentrated using the RNA Clean & Concentrator-5 Kit (Zymo Research, Irvine, CA). The same amount of concentrated IP RNA or input RNA from each sample was used for the cDNA library. Relative m⁶A levels in genes were calculated by using m⁶A levels normalized to the expression (input) of each gene (m⁶A IP) (3, 4).

Immunoblotting

Protein extracts were obtained by washing the cells once with PBS and resuspending in RIPA buffer (Thermo Scientific™) containing a Protease and Phosphatase Inhibitor cocktail (Thermo Scientific™); next, cells were sonicated. After quantifying protein concentrations using a BCA assays (Thermo Scientific™) samples were heated for 10 min at 70 °C. Protein abundance was analyzed by SDS-polyacrylamide gel electrophoresis and immunoblotting. Antibody information is shown in Supplementary Table S3.

Immunoprecipitation

For immunoprecipitation, cells were fixed with 0.4% formaldehyde for 10 min and then quenched with 200 mM Tris-HCl (pH7.5) for 30 min. Fixed cells were scraped with 1X lysis buffer (cell lysis buffer, #9803, Cell Signaling) containing 1% SDS and 5 mM EDTA, and then boiled at 95 °C for 5 min. The cell lysate was then added to 1X Lysis buffer and mixed well, sonicated, and then incubated with 30 unit/ml of DNase I for 1 h. After centrifuging, the supernatant was used for the following immunoprecipitation (IP) experiments. IP was performed at 4 °C for 1.5 h using Anti-FLAG® M2 Magnetic Beads (Sigma, M8823, 1:20), Anti-HA Magnetic Beads (Thermo Scientific™, #88836), or normal Rabbit IgG (12-370, MilliporeSigma), GFP (ab290, Abcam) Protein A/G Magnetic Beads (ThermoFisher). The beads were washed in 1X cell lysis buffer (Cell signaling, #9803). Protein was eluted with SDS sample buffer containing DTT and heated at 95 °C for 20 min and immunoblotting was performed. Secondary antibodies were used as follows: Rabbit Anti-Mouse IgG (Light Chain Specific) (D3V2A) (Cell Signaling, #58802, 1:2000), and Mouse Anti-Rabbit IgG (Conformation Specific) (L27A9) (HRP Conjugate) (Cell signaling, #5127 HRP, 1:2000).

Immunofluorescence

For tissue immunofluorescence staining, formalin-fixed, paraffin-embedded tissue sections first underwent antigen retrieval. Next, the sections were incubated with a blocking solution of 5% chicken serum (Jackson ImmunoResearch, 003-000-001) in PBS to prevent non-specific binding. The slides were then incubated with the primary anti-FTO antibody (Abcam, ab92821, diluted 1:200) overnight at 4°C. After incubation, the slides were washed with PBS containing 0.1% Triton X-100 (Sigma-Aldrich, T8787). Subsequently, the slides were incubated at room temperature for

1 hour with Alexa Fluor 448-conjugated secondary rabbit IgG (Jackson ImmunoResearch Lab, 715-545-150, diluted 1:200). The slides were then washed three times with PBS containing 0.1% Triton X-100. For mounting, the slides were covered with Prolong Gold Antifade reagent with DAPI to enable nuclear counterstaining. Fluorescence imaging of the stained slides was conducted using an Olympus IX71 microscope (Olympus Life Science, Japan). ImageJ was used for subsequent analysis.

Mass Spectrometric analysis of FTO-interacting proteins

HEK293T cells were transfected with EV-Flag and FTO-Flag constructs for 48 h. Cells were then treated with vehicle (dimethyl sulfoxide, DMSO, Sigma) or Vitamin E succinate (10 μ M; T3126; Sigma) for 24 h. Samples were prepared for mass spectrometry using a DYKDDDDK Fab-Trap™ Agarose kit (Chromotek) according to the manufacturer's instructions. Briefly, cells were first fixed with 0.4% formaldehyde for 10 min and then quenched with 200 mM Tris-HCl (pH 7.5) for 30 min. Next, the cells were suspended in RIPA buffer (10 mM Tris/Cl pH 7.5, 150 mM NaCl, 0.5 mM EDTA, 0.1 % SDS, 1 % Triton™ X-100, 1 % deoxycholate) supplemented with DNase I (150 Kunitz U/mL), MgCl₂ (2.5 mM), protease inhibitor cocktail, and PMSF (1 mM). The diluted lysate was then incubated with the equilibrated DYKDDDDK Fab-Trap™ Agarose for 2 h at 4°C. After washing twice, samples were eluted with 3x DYKDDDDK-peptide (ChromeTek, Cat# fp-1). Eluted protein samples were further processed and analyzed using mass spectrometry by the Mass Spectrometry and Proteomics Facility at the Ohio State University (Columbus, Ohio). Briefly, protein samples were digested via Strap, followed by drying in a vacufuge and resuspending in 0.1% formic acid in water for Liquid Chromatography with tandem mass spectrometry (LC-MS/MS) analysis. Nano-liquid chromatography-nanospray tandem mass spectrometry (Nano-LC/MS/MS) for protein identification was performed on a Thermo Scientific Orbitrap Fusion mass spectrometer equipped with a nanospray source equipped with a FAIMS Pro™ Interface operated in positive ion mode. Samples were separated on an easy spray nano column (Pepmap™ RSLC, C18 3 μ 100A, 75 μ m X150mm Thermo Scientific) using a 2D RSLC HPLC system from Thermo Scientific. Data were searched using Mascot Daemon by Matrix Science version 2.7.0 (Boston, MA) via ProteomeDiscoverer (version 2.4 Thermo Scientific,) and the database searched against the most recent Uniprot databases. Finally, the volcano plot and statistical analysis for FTO-interacting proteins were generated using the Scaffold Proteome software.

Ubiquitination assay

Cells were co-transfected with the indicated gene expression vectors and HA-tagged ubiquitin vector. Then cells were treated with MG132 (10 μ M) for 6 h. Ubiquitination assays were performed under denaturing conditions. Briefly, cells were scraped with 1X Cell Lysis Buffer (10X Cell Lysis Buffer, #9803, Cell Signaling) containing 2% SDS and 5 mM EDTA, then boiled at 95°C for 5 min. The cell lysate was incubated with 1X Lysis buffer to quench SDS in the harvest buffer, mixed thoroughly, and then sonicated. After centrifugation, lysates were immunoprecipitated with Anti-FLAG® M2 magnetic beads (Sigma, M8823), IgG, or anti-GFP antibodies. Proteins were then eluted with SDS sample buffer containing DTT and heated at 95 °C for 20 min. All buffers contained protease cocktail inhibitors and 5 mM NEM (N-ethylmaleimide). Ubiquitinated proteins were detected by immunoblotting using the anti-HA (C29F4) (Cell Signaling, #3724, 1:2000) or anti-ubiquitin antibodies (Santa Cruz, sc-8017, 1:500). Secondary antibodies were used as follows: Rabbit Anti-Mouse IgG (Light Chain Specific) (D3V2A) (Cell Signaling, #58802, 1:2000) and Mouse Anti-Rabbit IgG (Conformation Specific) (L27A9) (HRP Conjugate) (Cell signaling, #5127 HRP, 1:2000).

Flow cytometric analysis

Apoptotic cell death was determined using an annexin V-FITC apoptosis detection kit (eBioscience, San Diego), according to the manufacturer's instructions. Cell samples were then analyzed by a BD flow cytometer (FACS Calibur, LSR Fortessa, or LSRII, BD Biosciences).

Cell proliferation assay

Cell proliferation was assessed with a Cell Counting Kit-8 (CCK-8) (Sigma-Aldrich, St. Louis, MO) following the manufacturer's protocol.

Co-culture assay for human melanoma cells and human T cells

Human Primary T Cells were kindly provided by Dr. Justin Kline. Briefly, PBMCs were isolated from healthy adult blood donors. After monocytes were removed from the PBMCs, the suspended PBMC cells were collected. Next, primary human T cells were expanded and activated using TexMACS™ GMP Medium (Miltenyi Biotec. 170-076-307) with CD3/CD28 Dynabeads (Thermo Fisher, 11161D), IL-7 (5 ng/ml, PEPROTECH, 200-07), and IL-15 (5 ng/mL, PEPROTECH, 200-15) in 10% FBS. For co-culture experiments, MEL624 or WM35 cells were stably infected with lentiviral vectors followed by selection with Puromycin. After pre-treatment with or without VES for 72 hours, MEL624 and WM35 cells were directly mixed with T cells and co-cultured in 24-well plates for 48 h (1:1 for both the MEL624/T cell co-culture and the WM35/T cell co-culture). Next, cells were collected and mixed with absolute counting beads (C36950, Thermo Fisher Scientific; ACFP-70-10, Spherotech, Inc.) (7). The number of GFP+ cells was determined using flow cytometry. Data analysis was performed using FlowJo V10 Software.

Drug Affinity Responsive Targets Stability (DARTS) assay

For the Drug Affinity Responsive Targets Stability (DARTS) assay, cells were washed with 1X PBS, and then lysed in Lysis buffer (50mM Tris pH 7.5, 150mM NaCl, 10% Glycerol, 1% IGEPAL) containing Phosphatase and Protease Inhibitor Cocktail and EDTA. After centrifugation, the lysates were mixed with TNC buffer (500 mM Tris-HCl (pH 8.0), 500 mM NaCl, and 100 mM CaCl₂). The lysates were split into 5 samples by transferring 100 µl aliquots into 1.5 ml Eppendorf tubes, incubated with vehicle or VES at the indicated concentrations for 1 hour at room temperature, and then digested with Pronase (1:10000, 10165921001, Roche) for an additional 30 minutes at room temperature. The reaction was quenched by buffer containing SDS and DTT, and then incubated at 70°C for 10 min. Finally, immunoblotting was performed to determine whether FTO is a direct target of VES. GAPDH was used as a negative control (7, 8).

Cellular Thermal Shift Assay (CETSA)

For the Cellular Thermal Shift Assay (CETSA), cells were pretreated with vehicle or VES for 16 hours at 37°C in a CO₂ incubator. Cells were collected using trypsin and then carefully resuspended in 1 ml of PBS supplemented with protease. The cell suspension was distributed onto a PCR strip and then heated to the designed temperature endpoint using a Bio-Rad MJmini Personal Thermal cycle (Bio-Rad). Immediately after heating, the tubes were removed and then the samples were incubated at room temperature for 3 min. Next, the samples were immediately snap-frozen in liquid nitrogen. The cells were then subjected to two freeze-thaw cycles using liquid nitrogen and a heating block at 25 °C, followed by centrifugation at 20,000 g for 20 min at 4°C. Finally, the supernatant was boiled with sample buffer containing SDS and DTT for immunoblotting (7, 9).

RNA m⁶A demethylation assay in cell free system

The m⁶A demethylase assay was conducted using a m⁶A demethylase assay kit (ab233489, Abcam) following the manufacturer's protocol. Recombinant FTO protein was purchased from Active Motif (31572)⁵⁰.

Tumor-infiltrating immune analysis

For the tumor-infiltrating immune analysis, tumor tissues were dissected from euthanized tumor-bearing mice, minced into small pieces (≤ 2 mm) using a scalpel in a dish, and then transferred to a 14 mL round-bottom tube containing 5 mL tumor digestion medium (500 μ L Collagenase/Hyaluronidase Solution, 750 μ L 1 mg/ml DNase I Solution, and 3.75 ml RPMI 1640 Medium). After incubation at 37°C for 25 min on a shaking platform, the digested tumor tissues were transferred into a 70 μ m mesh nylon strainer on a 50 mL conical tube, pushed through the strainer using the rubber end of a syringe plunger, and rinsed with the recommended medium. After centrifugation at 300 x g for 10 min at room temperature with the brake on low, the resulting cell pellets were added to 10 mL of ammonium chloride solution for incubation at room temperature for 5 minutes, followed by centrifugation at 300 x g for 10 minutes at room temperature with the brake on low. The resulting cell pellets were re-suspended at $1-10 \times 10^6$ cells/mL in cell staining buffer (BioLegend, # 420201). Half of the cells were incubated with anti-mouse CD16/CD32 (Mouse BD Fc Block™) according to the manufacturer's instructions (BD Biosciences). After the final wash, 5×10^6 cells were stained with surface markers including CD45 (BV605), B220 (FITC), CD206 (APC), CD3 (BV421), CD4 (PE), CD8 (BV711), or PD-1 (APC-cy7) according to the manufacturer's instructions (BioLegend). The other half of the cells was re-suspended with RPMI 1640 Medium plus Cell Activation Cocktail (with Brefeldin A, BioLegend 423303) and incubated at 37°C for 4 hours. After incubation, subsequent surface marker (CD3 (BV421), CD4 (PE), CD8 (BV711)) staining was performed in Cell Staining Buffer. For intracellular staining of cytoplasmic proteins (TNF- α (FITC), IFN- γ (APC)), the Fixation/Permeabilization Solution Kit (BD Biosciences) was used according to the manufacturer's instructions. The gating strategy is shown in Supplementary Fig. S14.

RNA sequencing and data analysis

Total RNA was isolated using the RNeasy Plus Mini Kit (Qiagen) and RNA was purified after treatment with DNase for sequencing. After sequencing, FastQC (version 0.11.7) was used to assess sequencing quality. Trimmomatic (version 0.36) was used to remove adapters and filter reads (Phred score >33). Reads were then aligned to the reference genome (hg38) using STAR (version 2.6.1d). Picard (version 2.18.29) was used to mark and remove duplicate reads. FeatureCounts of Subread (version 1.5.3) was used to count aligned reads. All analyses were performed on the University of Chicago High Performance Computing Cluster, Gardner. The Differential gene expression (DEG) was performed by NetworkAnalyst (<http://www.networkanalyst.ca>), an R programming language-based tool for comprehensive gene expression profiling (10). The edgeR method was selected with adjusted $P < 0.05$ to identify the DEGs between VES and vehicle-treated MEL624 cells.

In situ proximity ligation (PLA) assay

PLA assay was performed according to the manufacturer's instructions (Sigma). Briefly, cells were fixed with 4% paraformaldehyde/PBS and then permeabilized in 0.5 % (v/v) Triton X-100. After blocking with 5% normal goat serum (Invitrogen, Carlsbad, California), cells were incubated overnight at 4 °C in 1XPBS/1%BSA containing the following primary antibodies: anti-DTX2 (thermofisher; PA5-60164) or anti-FTO (mouse) (Abcam, ab92821). In-situ PLA detection was performed using a Duolink Detection Kit (Sigma-Aldrich) with a pair of nucleotide-labeled secondary antibodies. After ligation and amplification of PLA probes, signals were examined using a fluorescence microscope (Olympus IX71).

TUNEL assay

TUNEL assay was performed using the Click-iT™ Plus TUNEL Assay Kits for In Situ Apoptosis Detection kit (Thermofisher, C10618) following the manufacturer's instructions.

Molecular docking

VES ligands were built using Chemdraw software and optimized using LigPrep in the Schrödinger 2018 software. The X-ray structure of FTO was downloaded from the Protein DataBank (PDB code 4IE6) and prepared with the Protein Preparation module. The docking grid was centered on the putative binding site, comprising ARG316, ASN205, TYR295, TYR205, ARG322, ASP233, and SER318, and the box size was set as 20 Å. The Induced Fit docking was performed according to the protocol in Schrodinger Suite 2018.

Pathway analysis, human database analysis and survival analysis

Gene ontology (GO) enrichment and Kyoto Encyclopedia of Genes and Genomes (KEGG) pathway enrichment analyses were performed using Metascape (<https://metascape.org/>) (11), a web-based portal designed to provide a comprehensive gene list annotation and analysis resource. Gene expression correlation analyses from human patients were performed using PINA v3.0 (<https://omics.bjcancer.org/pina/>) (12, 13) and UCSC Xena (<https://xenabrowser.net/>). Overall survival analyses were performed using KM Plot (<https://kmplot.com/analysis/>). Gene Set Enrichment Analysis (GSEA) and the heatmap of relative significant genes were created using WebGestalt (<http://www.webgestalt.org/>) (14).

Statistical analyses

Statistical analyses were carried out using Prism (GraphPad). Data were expressed as the mean of at least three independent experiments. Error bars indicate the SDs or SEs of the means. $P < 0.05$ was considered statistically significant.

References

1. M. P. Malafa, F. D. Fokum, A. Mowlavi, M. Abusief, M. King, Vitamin E inhibits melanoma growth in mice. *Surgery* **131**, 85-91 (2002).
2. J. Quin *et al.*, Vitamin E succinate decreases lung cancer tumor growth in mice. *J Surg Res* **127**, 139-143 (2005).
3. Y. H. Cui *et al.*, Autophagy of the m(6)A mRNA demethylase FTO is impaired by low-level arsenic exposure to promote tumorigenesis. *Nat Commun* **12**, 2183 (2021).
4. S. Yang *et al.*, m(6)A mRNA demethylase FTO regulates melanoma tumorigenicity and response to anti-PD-1 blockade. *Nat Commun* **10**, 2782 (2019).
5. J. Wei *et al.*, Differential m(6)A, m(6)A(m), and m(1)A Demethylation Mediated by FTO in the Cell Nucleus and Cytoplasm. *Mol Cell* **71**, 973-985 e975 (2018).
6. Z. Yang *et al.*, METTL14 facilitates global genome repair and suppresses skin tumorigenesis. *Proc Natl Acad Sci U S A* **118** (2021) e2025948118. doi: 10.1073/pnas.2025948118.
7. R. Su *et al.*, Targeting FTO Suppresses Cancer Stem Cell Maintenance and Immune Evasion. *Cancer Cell* **38**, 79-96 e11 (2020).
8. B. Lomenick, G. Jung, J. A. Wohlschlegel, J. Huang, Target identification using drug affinity responsive target stability (DARTS). *Curr Protoc Chem Biol* **3**, 163-180 (2011).
9. R. Jafari *et al.*, The cellular thermal shift assay for evaluating drug target interactions in cells. *Nat Protoc* **9**, 2100-2122 (2014).
10. G. Zhou *et al.*, NetworkAnalyst 3.0: a visual analytics platform for comprehensive gene expression profiling and meta-analysis. *Nucleic Acids Res* **47**, W234-W241 (2019).
11. Y. Zhou *et al.*, Metascape provides a biologist-oriented resource for the analysis of systems-level datasets. *Nat Commun* **10**, 1523 (2019).
12. Y. Du *et al.*, PINA 3.0: mining cancer interactome. *Nucleic Acids Res* **49**, D1351-D1357 (2021).
13. M. J. Cowley *et al.*, PINA v2.0: mining interactome modules. *Nucleic Acids Res* **40**, D862-865 (2012).
14. Y. Liao, J. Wang, E. J. Jaehnig, Z. Shi, B. Zhang, WebGestalt 2019: gene set analysis toolkit with revamped UIs and APIs. *Nucleic Acids Res* **47**, W199-W205 (2019).